FIZIKA, 4 (1969) 183–202

X-RAY DIFFRACTION STUDY OF THE PROCESS OF GRAPHITIZATION*

S. POPOVIĆ

Institute »Ruđer Bošković«, Zagreb

Received 18 November 1968; revised manuscript received 5 March 1969

Abstract: A series of samples of various crystallinity are obtained by heating of petroleum coke powder from 1000° C up to 3000° C. The temperature changes of the microstructural parameters are determined and the discussion about the gradual modulation of the diffraction lines during the process of graphitization is presented. By increasing the temperature above 1200° C the initial interlayer spacing d_{002} (3.47 Å) decreases to the value (3.44 Å) known as the spacing of the non-graphitic carbons. Above 1600° C d_{002} decreases very slowly and up to 2150° C the samples possess the random-layer structure. Above 2200° C the pairs of the nearest neighbour layers begin to take on the graphite relation and d_{002} abruptly decreases. The ordering produces modulations in the twodimensional (*hk*) bands with the appearance of (*hkl*) reflections.

A part of the volume retains the random-layer structure above 2200° C, without change of d_{002} and its proportion decreases from 15% at 2230° C to 5% at 3000° C. In the whole temperature range the dimensions of the parallel layer groups normal to the layers (L_c) and parallel to the layers (L_a) increase. The increasing of L_c and L_a is especially pronounced above 1900° C and 2200° C, respectively. The averaged lattice distortion decreases with the temperature increasing, and the decreasing is the most important from 1600° C to 2100° C. In the beginning, the ordering of nearest neighbour pairs depends on the other neighbouring layers. The distribution of oriented and disoriented layers in the crystallites of the graphitic component is random above 2200° C.

1. Introduction

Microstructural parameters of the non-graphitic and graphitic carbons and crystalline graphite have been investigated by many authors. The X-ray pattern of the non-graphitic carbon is higly diffuse and diffraction effects observed are only (002) and (004) reflections as well as twodimensional (10) and (11) bands of the type described by Warren[1]. Such pattern indicates that

* This work was partially reported at the 7th International Congress of Crystallographers, Moscow, 1966, under the title: »The absolute crystallite size and lattice distortion determination of graphitized petroleum coke«.

the carbon contains minute crystallites with graphitelike layers stacked roughly parallel but not otherwise mutually oriented[2, 3]. A part of the volume is in a much less organized state.

The conception of the graphitic carbons has been introduced by Franklin[4] for those carbons in which there are three-dimensional correlations between a number of graphite layers. Those correlations appear in the diffraction pattern as modulations of the (*hk*) bands. As a measure of ordering in graphitic carbons Franklin proposed the parameter p defined as the fraction of layers not showing three-dimensional graphite orientation. The oriented and disoriented layers are in approximately random distribution within the crystallites as the packets of parallel layers. Franklin[4] and Bacon [5, 6] found a nonlinear relationship between the average interlayer spacing d_{002} and p, and concluded that a model of oriented and disoriented stacks of layers with unique interlayer spacings corresponding to each type of ordering is too simple.

Houska and Warren[7, 8] introduced the parameter P_1 defined as the probability for the occurrence of correct graphite relation between two adjacent layers. They proposed the method for evaluation of P_1 using the Fourier analysis of the modulated (*hk*) diffraction profiles. According to Méring and Maire[9, 10] oriented stacks are considered to possess a unique spacing equal to that of a perfect graphite, 3.354 Å, whereas the disoriented stacks are supposed to have a constant mean spacing, equal to 3.44 Å.

Most recently Richards[11] presented a comprehensive review of all ordering parameters (introduced by Franklin, Bacon, Houska and Warren, Méring and Maire, Ruland[12] and found the relationships between them based on their definitions.

In the early stages of heat treatment of the carbonaceous substance the layer diameter grows and the number of layers in a parallel layer group increases, but the orientation of the layers about the layer normals remain random. The transition to the graphitic carbon occurs when the layer diameter gets above a certain size, which is of the order of 100 Å as suggested by Houska and Warren[7]. When the temperature further increases the ordering of the layers proceeds parallel to the crystallite growth. Richards[11] discussed the correlations which might be expected between the stacking order and the crystallite dimensions.

The present paper is concerned with a series of samples of various crystallinity prepared by heating of chemically purified petroleum coke powder up to 3000° C. The samples represent a gradual transition from the nongraphitic carbons towards the graphitic ones and the crystalline graphite. Although there are plenty of data concerning the changes of the microstructural parameters during the temperature treatment in the cited literature, we have hoped to throw some new light on them using somewhat different methods.

We have tried to answer the question: Does the interlayer spacing d_{002} slowly change from the initial value to 3.354 Å with the increase of temperature, or does it decrease abruptly at the beginning of the layer ordering? It is also of interest to explain the asymmetry of (00*l*) reflections mentioned by Franklin.[4]. If the asymmetry exists, is it due to a part of the volume which retains the random layer structure of non-graphitic carbons up to the highest temperatures of heating?

2. *The analysis of the broadening of X-ray diffraction line profiles*

Microstructural parameters of powders, as crystallite size, lattice distortion and faults, can be studied by the analysis of the X-ray diffraction line profiles corrected for the instrumental broadening. The instrumental weight function $g(\varepsilon)$ transforms the pure diffraction profile $f(\varepsilon)$ into the observed profile $h(\varepsilon)$ according to the convolution equation[13]:

$$h(\varepsilon) = \int_{-\infty}^{+\infty} f(\varepsilon - t)\ g(t)dt. \tag{2.1}$$

Here both ε and t represent the angular deviation from the position of the peak maximum $2\Theta_0$. Stokes[14] has shown how the desired function $f(\varepsilon)$ can be obtained from the observed profiles $h(\varepsilon)$ and $g(\varepsilon)$ *by* making use of the Fourier transform theory. That procedure is by far the most comprehensive one and has the advantage of yielding immediately the Fourier coefficients of $f(\varepsilon)$. As shown by Warren and Averbach [15-18] and also by Bertaut[19] the profile $f(\varepsilon)$ or $f(2\Theta)$ can be expressed in terms of a Fourier series

$$f(2\Theta) \propto \sum_{L=-\infty}^{+\infty} F(L, l)\ \exp\left[-i\,2\pi\,L\,\frac{2}{\lambda}\,(\sin\Theta - \sin\Theta_0)\right],$$

where L is a distance normal to the reflecting planes (00*l*) with the interplanar spacing d_{00l}, and λ is the wavelength of X-rays.

For simplicity we consider only those (00*l*) reflections, which are free from the broadening due to the layer stacking faults. Acording to Wilson[20] (pp. 67–74), Warren[18] and also to Wagner and Aqua[21] hexagonal reflections are not broadened due to the existence of the rhombohedral stacking sequences ABC within the regular hexagonal ABAB arrangement, if $|h-k| = 3N$, where N is an integer. Such graphite reflections are (002), (004), (110), (112), etc.

Fourier coefficients are given by

$$F(L, l) = F_p(L) \cdot F_s(L, l) ,$$

where $F_p(L)$ and $F_s(L, l)$ are crystallite size and lattice distortion coefficients, respectively. The initial slope of the $|F_p(L)|$ vs. L curve is a measure of the mean crystallite size $\langle L_c \rangle$ in the direction along the c axis, normal to the reflecting plane $(00l)$:

$$\left.\frac{d|F_p(L)|}{dL}\right|_{L=0} = -\frac{1}{\langle L_c \rangle} . \tag{2.2}$$

Regardless of the nature of the strains, providing only that they remain finite, the distortion coefficients are given by[17]

$$|F_s(L, l)| = \exp\left[-2\pi^2 c^{-2} \left\langle (\Delta L)^2_L \right\rangle l^2\right] \tag{2.3}$$

where c is unit cell dimension ($c = l d_{00l}$) and $\langle (\Delta L)^2_L \rangle$ is the mean square change of the distance L normal to planes $(00l)$ due to distortion. Since the coefficients $F_s(L, l)$ depend on l, they can be separated from $F_p(L)$ by plotting $\ln |F(L, l)|$ as a function of l^2 and extrapolating to $l^2 = 0$, if at least two reflections $(00l)$ are available.

The pure diffraction profile $f(\varepsilon)$ is the convolution of the crystallite size profile, $p(\varepsilon)$, and the lattice distortion profile, $s(\varepsilon)$, according to the equation analogous to (2.1) If β_{pi} and β_{si} are the integral breadths of the profiles $p(\varepsilon)$ and $s(\varepsilon)$, respectively, the resultant integral breadth β_i of the $f(\varepsilon)$ is given by[13]

$$\beta_i = \frac{\beta_{pi}\, \beta_{si}}{p(\varepsilon) s(\varepsilon) d\varepsilon} . \tag{2.4}$$

In order to find the relationship between β_i, β_{pi} and β_{si} one must assume analytical functions for $p(\varepsilon)$ and $s(\varepsilon)$[22-27]. Such assumptions, however, affect the final result of the separation of the line broadening effects. Solving two equations (2.4), for two hexagonal reflections $(00l)$, with integral breadths β_{i_1} and β_{i_2}, respectively, one can obtain the expressions for the crystallite size L_c normal to the reflecting planes and for the corresponding distortion component e using the well known formulae:[26, 28]

$$L_c = \lambda/(\beta_{pi} \cos\Theta_0), \qquad e = \beta_{si}/(4 \operatorname{tg}\Theta_0).$$

3. *Experimental*

The samples were prepared by heating of petroleum coke powder (produced by Great Lakes Carbon Corp. USA) of granulation from 140 to 160 mesh in a laboratory furnace for 30 minutes in the atmosphere of argon. It was possible to reach any predetermined temperature in less than one minute. It is known that the microstructural parameters are also a function of the holding time at the given temperature. Mason and others have found that the changes do not cease even after 2 hours of heating[29]. According to Mrozowski[30], however, the main changes occur in the first state of heating (in the first 10 or 20 minutes, or so) after the top temperature is reached. In our experiments we have not seen any significant difference between the samples heated for 20 and 30 minutes, respectively.

X-ray diffraction patterns were recorded by a method of fixed time couting, at uniformly spaced angular intervals on a Philips diffractometer with a scintillation counter and a single channel pulse height analyser, using filtered Cu Kα radiation. Bragg angles were determined by the method of mixing the examined samples with standards whose unit cell dimensions were previously accurately obtained. For the standards germanium and silicon powders of high purity and a very regular crystal lattice were selected ($a_{Ge} = 5.6575$ Å, $a_{Si} = 5.4305$ Å at 25° C). Germanium and silicon (111), (311) and (331) diffraction lines are located close to measured graphite lines and the equallity of the instrumental errors for two neighbouring lines of both samples can be assumed. As the standard for (002) graphite reflection it is more appropriate to use (111) germanium reflection than (111) silicon reflection. But for the samples heated up to 1800° C (002) reflections are very broad and it is better to use (111) silicon reflection. The position of (004) reflection was always corrected using (311) silicon reflection. For (110) and (112) graphite reflections we always used (331) germanium reflection. The same diffractometer records were also used for the correction of the line profiles for the instrumental broadening by the method of Stokes[14]. According to X-ray pattern of the homogeneous mixture of germanium and silicon it was evident that the profiles of germanium reflections were quite equal to the corresponding silicon reflections, with the same indices h, k, l. Therefore it was possible to use alternatively germanium and silicon as standards for (002) and (004) reflections. Fourier intervals of the profiles $[2\Theta_{+M}, 2\Theta_{-M}]$ (where $2\Theta_{+M} - 2\Theta_0 = 2\Theta_0 - 2\Theta_{-M}$), selected large enough to include the measurable tails of the profiles, were divided into 160 or 320 intervals. The Fourier coefficients $H(t) = H_r(t) + iH_i(t)$ of the resultant profile $h(\varepsilon)$ and the coefficients $G(t) = G_r(t) + iG_i(t)$ of the instrumental profile $g(\varepsilon)$ were determined using a CAE 90-40 computer. As shown by Stokes the pure diffraction profile coefficients are:

$$F(t) = F_r(t) + iF_i(t) = \frac{H(t)}{G_1^2(t)},$$

which were used for the synthesis of $f(\varepsilon)$.

The pure diffraction integral breadths were calculated using the coefficients $|F_r(0)|$ and the maximum heights $f(0)$ according to the equation

$$\beta_i = \frac{|F_r(0)|}{f(0)} (2\Theta_M - 2\Theta_{-M}). \tag{3.1}$$

The crystallite size normal to the layers and the corresponding lattice distortion component were determined by the method of Warren and Averbach [equations (2.2) and (2.3)], using the coefficients $|F(t)|$ of the reflections (002) and (004). These coefficients were transformed into $|F(L,l)|$ according to formula[17]

$$L = \frac{\lambda t}{2(\sin\Theta_M - \sin\Theta_{-M})}.$$

The analogous parameters, L_c and e, were also determined by assuming analytical functions$(1 + k_p^2 \varepsilon^2)^{-1}$ and $\exp(-k_p^2 \varepsilon^2)$ for $p(\varepsilon)$, and $(1+k_s^2 \varepsilon^2)^{-2}$ and $\exp(-k_s^2 \varepsilon^2)$ for $s(\varepsilon)$, using the integral breadths of the reflections (002) and (004) calculated according to (3.1).

The layer diameters L_a of the non-graphitic carbons (the samples heated up to 2200° C) were deduced from the half-maximum breadths $\beta_{1/2}$ of the asymmetrical two-dimensional reflections (10) and (11) according to the equation[1]

$$L_a = \frac{1.84\lambda}{\beta_{1/2}\cos\Theta_0}.$$

The background lines for (10) and (11) reflections were estimated by the method proposed by Houska and Warren[7, 8]. The samples were mixed with germanium in order to increase the absorption and so to minimize the instrumental broadening. As (10) and (11) reflections were very broad it was not necessary to make the corrections for other instrumental causes of broadening.

For graphitic carbons L_a was calculated from Scherrer's equation $L_a = \lambda/(\beta_i \cos\Theta_0)$ using the integral breadth β_i of the reflection (110) given by (3.1) We did not use the reflection (100) because it could not be separated accurately from the neighbouring rhombohedral reflection $(10\frac{2}{3})$ (indices related to the hexanogal unit cell) and very broad reflection (101).

According to our earlier analysis of doublet separation broadening[31] we used the positions of the centres of gravity and the mean doublet wavelength ($\lambda = 1.5418$ Å for Cu Kα) in measuring the Bragg angles (except in the cases when the lines were clearly resolved in two components). The positions of the centres of gravity of the lines $h(\varepsilon)$ and $g(\varepsilon)$ were obtained also by the electronic computer using the same input data as for the Fourier coefficients.

The form of the two-dimensional reflections (10) and (11) and their gradual modulation with the increase of temperature are shown in Fig. 1 and

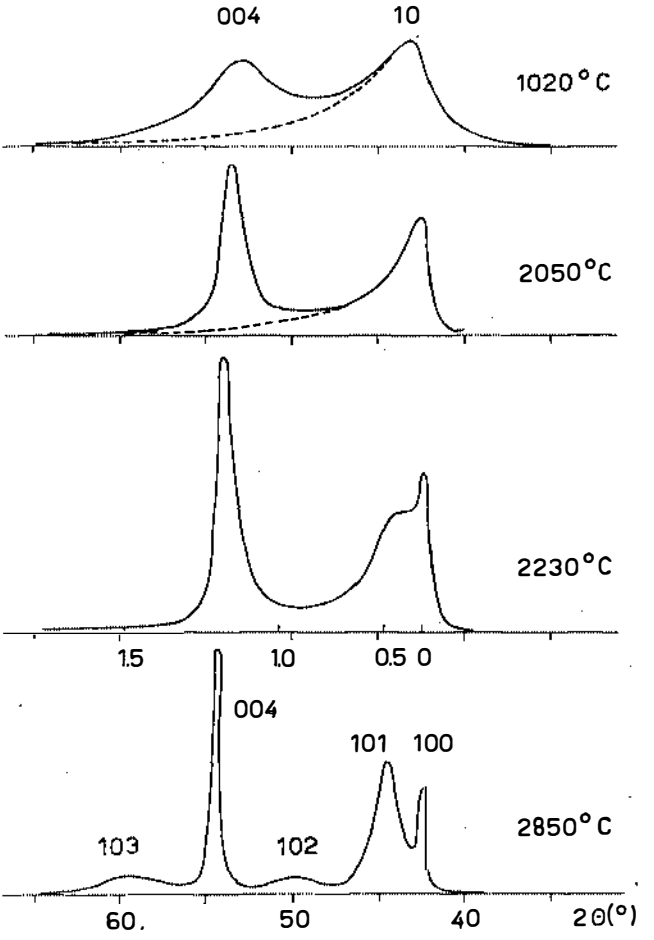

Fig. 1. The parts of the X-ray patterns for several samples heated at the various temperatures. One can see the modulation of the two-dimensional reflection (10) with the increase of the temperature.

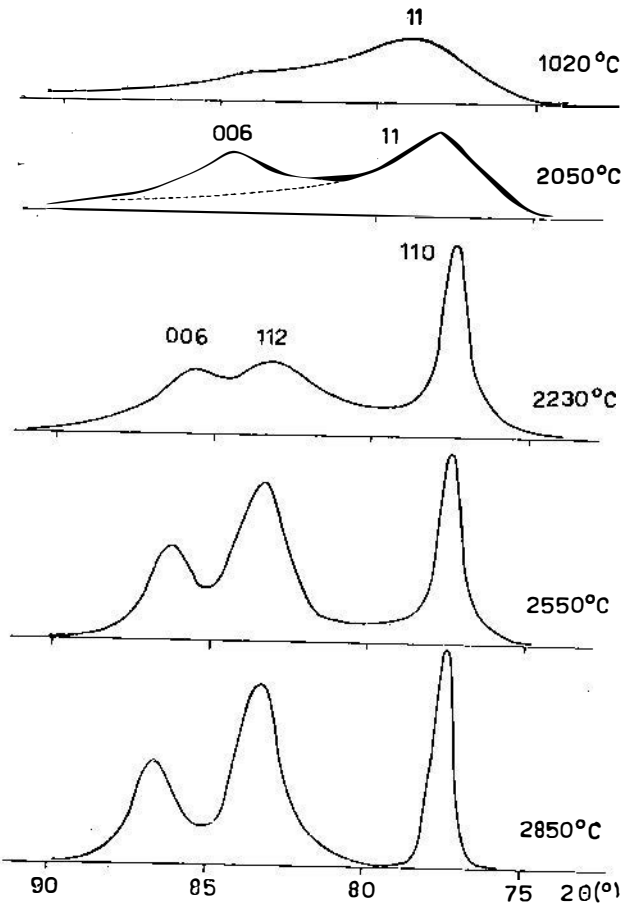

Fig. 2. The parts of the X-ray patterns for several samples heated at the various temperatures. One can see the modulation of the two-dimensional reflection (11) with the increase of the temperature.

2. Figures 3 to 6 represent the observed profiles $h(\varepsilon)$ and $g(\varepsilon)$ (full lines) and the pure diffraction profiles $f(\varepsilon)$ (broken lines) obtained by Stokes' method (for several temperatures). The variations of d_{002}, L_a and $\langle L_c \rangle$ with the heat treatment temperature are represented in Fig. 7, 8 and 9, respectively. The changes of the root mean square distortion $\langle (\Delta L)_L^2 \rangle^{1/2}$ with L (along the c axis) for several samples are shown in Fig. 10. The temperature change of the relative lattice distortion $\langle e \rangle$, defined as

$$\langle e \rangle = \frac{\left\langle (\Delta L)_L^2 \right\rangle^{1/2}}{L} \tag{3.2}$$

and calculated from the initial slopes of the curves in Fig. 10, is shown in Fig. 9. That figure also shows the temperature variation of the crystallite size L_c^S obtained from the Scherrer equation using the integral breadths β_i calculated from the equation (3.1) of the (002) reflections, and neglecting the broadening due to lattice distortion.

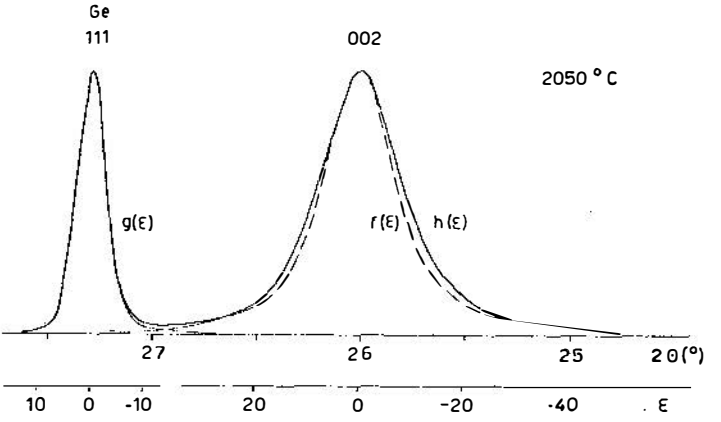

Fig. 3.

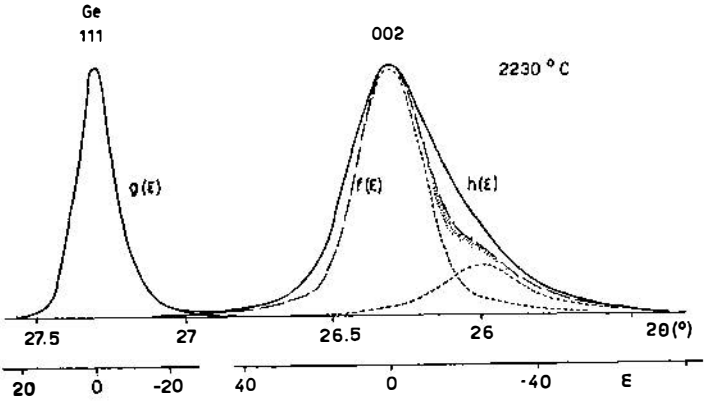

Fig. 4.

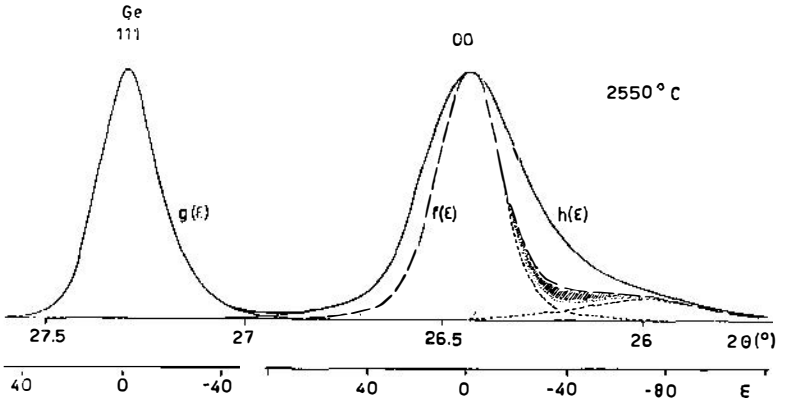

Fig. 5.

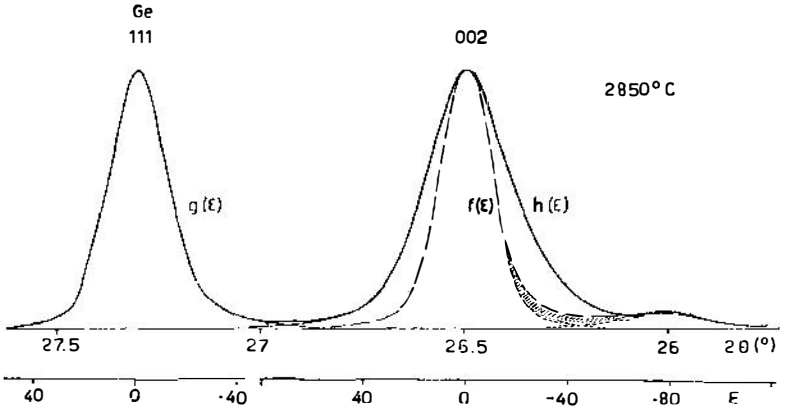

Fig. 6.

4. *Results and discussion*

4.1 The changes of the diffraction pattern during the temperature treatment. Untreated petroleum-coke is made up of minute crystallites in which there are several (about ten) roughly parallel graphite-like layers (with diameters of the order of 40 Å) but with random orientation about the layer normals. A part of the volume is in a much less organized state forming a disordered matrix surrounding the crystallites (according to Mrozowski[30] a great deal of the disordered phase is exhausted around 1300° C). The interlayer spacing is somewhat larger (3.47 Å) than for the non-graphitic carbons, as defined by Franklin (3.44 Å). The X-ray pattern consists only of broad (00*l*) crystalline reflections (002) and (004), and of asymmetrical (*hk*) bands (10) and (11). Above 1200° C diffraction pattern begins to change (Fig. 1 and 2). The (*hk*) reflections sharpen considerably, but retain the characteristic

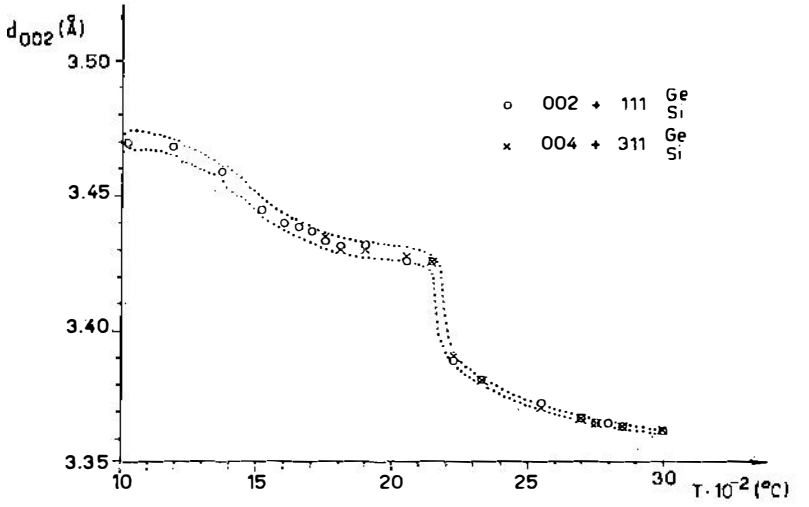

Fig. 7. The variation of the interlayer spacing d_{002} with the heat treatment temperature.

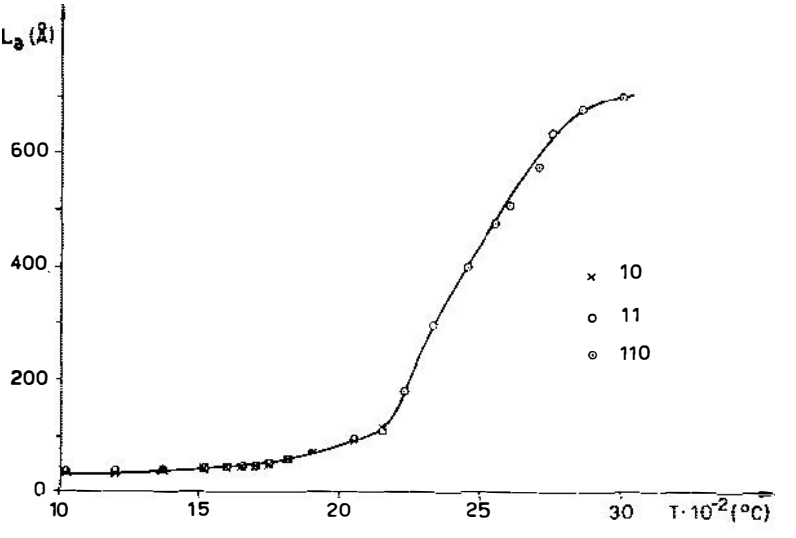

Fig. 8. The variation of the crystallite size L_a with the heat treatment temperature.

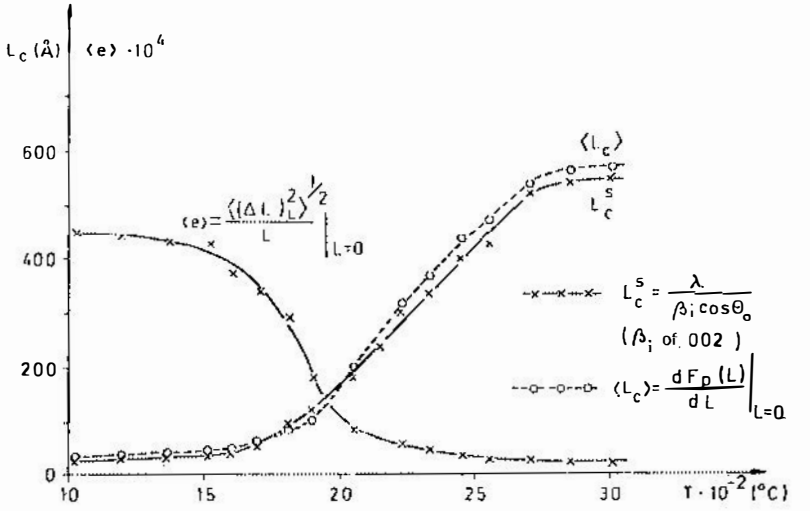

Fig. 9. The variations of $\langle L_c \rangle$ (determined by the method of Warren and Averbach), L_c^s (calculated from Scherrer's equation) and the relative distortion $\langle e \rangle$ with the increase of the heat treatment temperature.

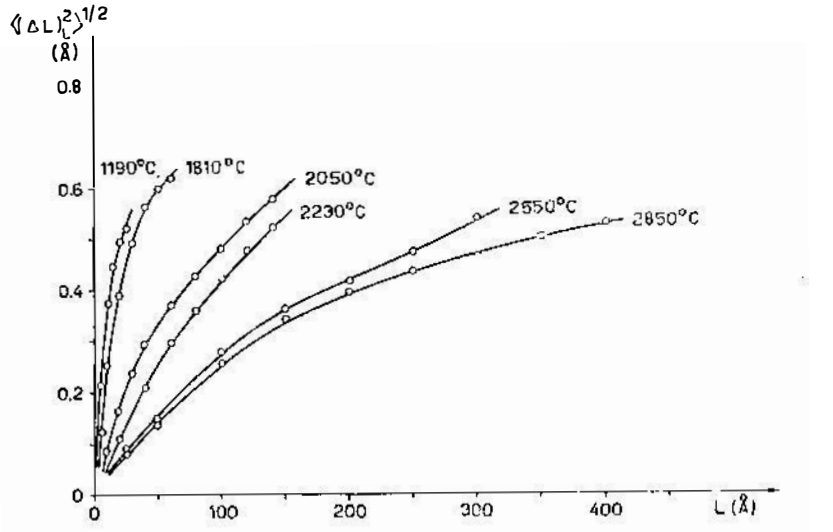

Fig. 10. The changes of the root mean square distortion along the c axis.

asymmetrical shape, indicating that the layer diameters increase; however, layers are further in random orientation about their normals. The positions of the peaks of the (*hk*) reflections move towards the smaller Bragg angles. That is in agreement with Warren's formula[1] for the displacement of the peaks of the (*hk*) reflections of the random layer structure when the layer diameter increases. The symmetrical (00*l*) reflections also sharpen, when the temperature raises, indicating an increase in the average number of layers in the crystallites. The sharpening of the (00*l*) reflections is especially pronounced in the temperature interval from 1500° C to 1900° C. Above 1600° C very broad reflection (006) also appears in the X-ray pattern. The interlayer spacing d_{002} decreases to the value 3.44 Å when the temperature reaches 1500° C. When the temperature further increases d_{002} changes more slowly. For the sample heated at 1900° C d_{002} is equal to 3.430 Å, and for the sample heated at 2150° C d_{002} is equal to 3.425 Å.

Diffraction patterns of all samples heated up to 2200° C are characteristic patterns of the non-graphitic carbons. But the pattern of the next sample, heated at 2230° C, is essentially different: it shows the beginning of the splitting of the reflection (10) into (100) and (101), and the reflection (11) into (110) and (112) Fig. 1 and 2). The appearance of modulations in the (*hk*) diffraction bands indicates the start of the graphitization. The nearest neighbouring layers, reaching the diameter of the order of 100 Å (what is in agreement with the results of Franklin and Warren) begin to take on the correct graphite relation. Simultaneously, with the beginning of modulations, the interlayer spacing d_{002} abruptly decreases (Fig. 7).

The pure diffraction profiles $f(\varepsilon)$ of the reflections (002) and (004) of the samples heated above 2200° C are asymmetrical (Fig. 4–6). The asymmetry is in the form of the evident doublet for the sample heated at 2550° C (Fig. 5). The doublet form is still more obvious for the samples heated at higher temperatures (Fig. 6). The stronger doublet component moves towards higher Bragg angles when the temperature increases. That component corresponds to the part of the volume in which the ordering of the layers takes place above 2200° C and therefore, it has the structure of graphitic carbon. Much weaker component retains in the whole temperature range above 2200° C the same angular position: $2\Theta_{002} = 26.01^0$, and $2\Theta_{004} = 53.52^0$, this corresponds to the interlayer spacing (3,425 Å) of the sample heated at 2150° C. Thus one can conclude that above 2200° C a part of the volume retains random layer structure up to 3000° C without change of its interlayer spacing.

The separation of the profiles $f(\varepsilon)$ of the reflections (002) and (004) into the graphitic and non-graphitic components is done under the following assumptions:

1) the both components should be symmetrical;

2) high angle side of the profile $f(\varepsilon)$ belongs completely to the graphitic component (except for the sample heated at 2230° C);
3) the position of the maximum of the graphitic component coincides with the maximum of $f(\varepsilon)$; and
4) the position of the non-graphitic component is constant.

The procedure of the separation is facilitated by the comparison of the profiles of two reflections. The assumption (1) we may introduce because of two facts: the profiles $f(\varepsilon)$ up to 2150° C are quite symmetrical, and the upper parts of the profiles $f(\varepsilon)$ of the samples heated above 2550° C are also symmetrical (these parts belong to the graphitic component). The assumptions (2) and (3) are proposed because the graphitic component is much more intensive than the non-graphitic one. The ratio of the integrated intensities of the components is about 6 at 2230° C, and about 20 at 2850° C. We could not obtain the clearly visible maximum of the non-graphitic component (even for the sample heated at 3000° C) when we did not use the mixture method with standard. In such case the both components, the graphitic and non-graphitic one, are additionally broadened due to the small absorption.

The profiles of the graphitic and non-graphitic components are shown in Fig. 4–6 by the shorter dashed lines.

The non-graphitic component has the random layer structure and one can expect [besides (00*l*) reflections] only its twodimensional bands (10) and (11). As the proportion of the non-graphitic component is small (especially above 2500° C) these bands are much weaker than the *(hkl)* reflections of the graphitic component, and practically they do not arise above the background line.

The doublet form of the pure diffraction profiles $f(\varepsilon)$ of the reflections (002) and (004) is especially evident for the samples heated at 2700° C, 2850° C and 3000° C. For these samples one can separate the graphitic component from the non-graphitic one with a great reliability. However, the sum of the graphitic and non-graphitic components (denoted in Fig. 4–6 with the arrows of points) in the angular range between them, is somewhat smaller than the ordinates of $f(\varepsilon)$. It seems that there is still one component in the samples, and it appears in all samples heated above 2200° C. The separation of the profiles of that component is very difficult and inaccurate, but it is almost evident that its integrated intensity increases with the temperature to 2550° C and then decreases above 2550° C For all samples the intensity of that third component (shown in Fig. 4-6 by shaded areas) is smaller than the intensity of the non-graphitic component. It seems that the non-graphitic component partially transforms to the graphitic one also through that third phase.

4.2 The microstructural parameters. According to the above discussion we hope that he graphitic component profiles (002) and (004) are separated with a reasonable accuracy. Using the high angle side of the graphitic component

profiles we determined the corresponding Fourier coefficients $|F(L, l)|$, the crystallite size $\langle L_c \rangle$, and lattice distortion $\langle (\Delta L)_L^2 \rangle^{1/2}$ values by the method of Warren and Averbach. The data for the interlayer spacing (in Fig. 7), crystallite size (in Fig. 9 and Table 1) and distortion (in Fig. 9 and 10 and Table 1) for the samples heated above 2200° C are related only to the graphitic component. Integral breadths of the graphitic component profiles were calculated according to the equation (3.1). The interlayer spacing values were determined from the positions of the maxima of the graphitic component lines [which coincide with the maxima of $f(\varepsilon)$] after correction for the instrumental displacement. The correction was done for (002) reflections using the centre of the gravity of the neighbouring (111) germanium reflection, and for (004) reflection using the positions of the separated doublet components of the (311) silicon reflection. In both cases, for the position of the maximum of the graphitic profile and for the position of the centre of gravity of (111) germanium line, we used the mean wavelength.

The variation of $\langle (\Delta L)_L^2 \rangle^{1/2}$ with L shown in Fig. 10 represents the lattice distortion which is present in the samples. It is seen that $\langle (\Delta L)_L^2 \rangle^{1/2}$ is not a linear function of L. But for all samples $\langle (\Delta L)_L^2 \rangle$ has a linear relationship with L, this is in agreement with Bowman's results[32]. Considering the model of Franklin[4] for the types of the interlayer spacings in the graphitic carbons Bowman showed that the linear change of $\langle (\Delta L)_L^2 \rangle$ with L is of the expected behaviour. The assumption included is that the ordering of the nearest neighbour layers is statistically independent of neighbouring layers. If it is assumed that the ordering of the nearest neighbour pairs is in some correlation with other neighbouring layers, then one can expect the linear change of $\langle (\Delta L)_L^2 \rangle^{1/2}$ with L over the short averaging distances L. The form of the curves in Fig. 10 indicates that the lattice distortion is not uniform but random localized within the crystallites.

Table 1 lists the following parameters:

1) the values of crystallite size $\langle L_c \rangle$ and relative lattice distortion $\langle e \rangle$ [calculated from the initial slopes of the curves in Fig. 10 according to the equation (3.2)], determined by the method of Warren and Averbach;

2) the values of L_c and e deduced from the integral breadths of the reflections (002) and (004) under the assumptions of various analytical functions for the dispersion and distortion profiles, as indicated; and

3) the value of L_c^S obtained from the Scherrer's equation using the integral breadhts of the (002) reflections and neglecting the distortion broadening.

Although the parameters $\langle L_c \rangle$ and L_c^S are not directly comparable (with respect to their definitions), it is of interest to note that they are very similar. One would have obtained much smaller values for L_c^S, if the integral breadths of the reflections (004) had been used. The distortion broadening is considerably bigger for the reflection of higher order.

Table 1

The microstructural parameters of the graphitized petroleum coke

heat treatment temperature (°C)	the method of Warren and Averbach		Scherrer's equation	$p(\varepsilon)=\exp(-k_p^2\varepsilon^2)$ $s(\varepsilon)=\exp(-k_s^2\varepsilon^2)$		$p(\varepsilon)=(1+k_p^2\varepsilon^2)^{-1}$ $s(\varepsilon)=\exp(-k_s^2\varepsilon^2)$		$p(\varepsilon)=(1+k_p^2\varepsilon^2)^{-1}$ $s(\varepsilon)=(1+k_s^2\varepsilon^2)^{-2}$	
	$\langle L_c\rangle$(Å)	$\langle e\rangle\cdot 10^2$	L_c^S(Å)	L_c(Å)	$e\cdot 10^2$	L_c(Å)	$e\cdot 10^2$	$\langle L_c\rangle$(Å)	$e\cdot 10^2$
1020	30	4.5	28	42	4.5	48	3.9	59	3.9
1190	32	4.4	29	43	4.5	53	3.9	65	3.8
1370	38	4.3	32	56	4.3	75	4.0	100	4.1
1520	42	4.3	37	100	4.3	260	4.2	360	4.4
1600	48	3.7	40	90	3.8	145	3.6	195	3.7
1700	65	3.4	52	135	3.1	295	2.9	410	3.0
1810	85	2.9	95		2.3		2.7		
1900	105	1.8	120		1.6		1.7		
2050	200	0.82	180	360	0.85	565	0.76	730	0.80
2230	320	0.55	300		0.59		0.60		
2330	365	0.48	330		0.50		0.49		
2550	435	0.28	420	670	0.31	740	0.29	1080	0.27
2700	540	0.30	520		0.30		0.28		
2850	565	0.26	540	930	0.25	1270	0.24	1600	0.23
3000	570	0.25	540	940	0.25	1280	0.24	1600	0.23

Table 1 also shows that the values of $\langle e\rangle$ are very close to the values of e deduced by the methods of assuming analytical functions for the dispersion and distortion profiles. On the other hand L_c values differ essentially from the values $\langle L_c\rangle$ depending on the function which is assumed for the dispersion profile. The approximation of the dispersion and distortion profiles by the Gaussian function gives the values L_c about two times bigger than $\langle L_c\rangle$ [what is in agreement with the results of other authors[21,25,26,28,33]]. The empty places in Table 1 mean that in these cases it is not adequate to apply the corresponding procedure and deduce L_c and e, because $\gamma_2 = (\beta_i \cos\Theta_o)_{004}$ is very close to $2\gamma_1$, $= 2(\beta_i \cos\Theta_o)_{002}$. If γ_2 is somewhat bigger or smaller than $2\gamma_1$, one obtains quite unadequate values for L_c and e.

The variation of the ratio $L_a / \langle L_c\rangle$ (or L_a/L_c^S) with the temperature for our samples is very similar to the plot given by Richards[11] (p. 46 Fig. 5b). According to Richards now it is believed that long range order in graphitizing carbons is established during the initial pyrolisis stages of the carbons. The long range order may be of a mosaic nature similar to that proposed by Steward

and Cook[34]. If general cylindrical shapes are assumed for the crystallites then the variation of the ratio $L_a/\langle L_c \rangle$ suggests that initially the crystallites are very small graphitelike platelets, which become more columnar with heat treatment as the mosaic substructure is established. At high temperatures the crystallites finally reassume their initial shape as the »columnar« crystallites coalesce within the mosaic which tends to the single-crystal condition (Richards[11]).

In the model presented by Heidenreich, Hess and Ban[35] the layer planes are bended from one crystallite to another rather than separate crystallites meeting at an angle. Thus L_a values would be considerably larger than those indicated by X-ray diffraction.

4.3 The stacking of layers. In order to confirm the random distribution of the disoriented layers in the graphitic component of the samples heated above 2200° C we have followed the method of Franklin[4]. The profiles of the reflections (112), corrected for the instrumental broadening by the method of Stokes, were compared with the theoretical profiles obtained by the formula of Hendricks and Teller[36]. The values of p were determined from the interlayer spacings d_{002}. The shapes of the experimental profiles were very similar to the theoretical profiles.

We have also been analysing the beginning of the modulation of twodimensional reflections (10) and (11) at 2230° C by the method proposed by Houska and Warren in order to determine the probabilities P_1, P_2^0 and P_2; P_1 is the probability of nearest neighbour layers being ordered, P_2^0 is the probability of second neighbour layers being in the ABA sequence, and P_2 is the probability of second neighbour layers being in the ABC sequence. The ordinates of (10) and (11) curves, corrected for the instrumental broadening, were divided by the terms preceding the summation in Warren's equation which describes the shapes of the modulated (hk) reflections[8]. The Fourier coefficients $A(n, hk)$ were determined using the half period from $h_3=0.5$ to $h_3=1.0$ (see Fig. 1) divided in 80 intervals [h_3 is defined as $\left(\frac{2d_{002}}{\lambda}\right)(\sin^2\Theta - \sin^2\Theta_0)^{1/2}$] and the following values were obtained:

$P_1 = 0.30$ [the mean value between $A(1, 10)$ and A(1, 11)],
$P_2^0 = 0.11$,
$P_2 = 0.08$.

Within the limits of the experimental error we may conclude that for the sample heated at 2230° C one third of the nearest neighbour pairs are ordered, and about one fifth (0.11 + 0.08) of the second neighbour pairs are ordered. For the latter there is somewhat higher probability for ABA sequence than for ABC one. Since the coefficients do not satisfy the relation $A(n, hk) =$

$= [A\,(1, hk)]_n$ the nearest neighbour pairs are not ordered quite independently of neighbouring layers. This is different from Warren's conclusion[8] for the early stage of graphitization of carbon black, which is non-graphitizing material.

Acknowledgement

The Author is very indebted to Dr K. Kranjc and Prof. S. Šćavničar (Faculty of Science, University of Zagreb) and also to Dr. B. Matković (Institute R. Bošković, Zagreb) for their advices and encouragement during this work. The author is also very grateful to Dr. B. P. Richards (The General Electric Company Ltd., Hirst Research Centre, Wembley, England) for a number of helpful discussions during the preparation of this paper.

References

1) B. E. Warren. Phys. Rev. 59 (1941) 693;
2) J. Biscoe & B. E. Warren. J. Appl. Phys. 13 (1942) 364;
3) R. E. Franklin. Acta Cryst. 3 (1950) 107;
4) R. E. Franklin. Acta Cryst. 4 (1951) 253;
5) G. E. Bacon. Acta Cryst. 4 (1951) 558;
6) G. E. Bacon. Atomic Energy Research Establishment, Harwell (1958) Report M/R 2702;
7) C. R. Houska & B. E. Warren. J. Appl. Phys. 25 (1954) 1503;
8) B. E. Warren »Proc. 1st & 2nd Carbon Conf.«, Pergamon Press, New York. (1956) 49;
9) J. Maire & J. Méring. »Proc. 1st Conf. Ind. Carbon & Graphite«, Society of Chemical Industry, London. (1958) 204;
10) J. Méring & J. Maire. J. Chim. Phys. 57 (1960) 803;
11) B. P. Richards. J. Appl. Cryst. 1 (1968) 35;
12) W. Ruland. Acta Cryst. 18 (1965) 992;
13) F. W. Jones. Proc. Roy Soc. A 166 (1938) 16;
14) A. R. Stokes. Proc. Phys. Soc. (London) 61 (1948) 382;
15) B. E. Warren & B. L. Averbach. J. Appl. Phys. 21 (1950) 595;
16) B. E. Warren Y B. L. Averbach. J. Appl. Phys. 23 (1952) 497, 1059;
17) B. E. Warren. Acta Cryst. 8 (1955) 483;
18) B. E. Warren. »Progress in Metal Physics« 8 (1959) 147;
19) M. F. Bertaut. C. R. Acad. Sci. Paris. 228 (1949) 492;
20) A. J. C. Wilson. »X-Ray Optics«, Methuen & Co. London (1949);
21) C. N. J. Wagner & E. N. Aqua. J. Less-Common Metals. 8 (1965) 51;
22) L. I. Lysak. Sb. trudov Lab. Metallofiz. AN USSR »Voprosi fiziki metallov i metallovedenija«. 5 (1954) 45;
23) F. R. L. Schoening. Acta Cryst. 18 (1965) 975;
24) G. V. Kudryumov & L. I. Lysak. J. Theor. Phys. U. S. S. R. 17 (1947) 993;
25) N. C. Halder & C. N. J. Wagner. Acta Cryst. 20 (1966) 312;
26) N. C. Halder & C. N. J. Wagner. »Advances in X-Ray Analysis«. 9 Plenum Press, New York. (1966) 91;
27) E. N. Aqua. Acta Cryst. 20 (1966) 560;
28) C. N. J. Wagner & E. N. Aqua. »Advances in X-Ray Analysis«. 7 Plenum Press, New York. (1963) 46;
29) I. B. Mason, E. A. Kellet, B. P. Richards, »Proc. 2nd Conf. Ind. Carbon and Graphite«, Society of Chemical Industry, London (1966) 159;
30) S. Mrozowski, »Kinetics of high temperature processes«, John Wiley & Sons, Inc. New York. (1959) 264;

31) S. Popović. Croat. Chem. Acta 39 (1967) 217;
32) J. C. Bowman. »Proc. 1st & 2nd Carbon Conf.« Pergamon Press, New York. (1956) 59;
33) G. B. Mitra & N. C. Halder, Acta Cryst. 17 (1964) 817;
34) E. G. Steward & B. P. Cook. Z. Kristalogr. 114 (1960) 245;
35) R. D. Heidenreich, W. M. Hess & L. L. Ban. J. Appl. Cryst. 1 (1968) 1;
36) S. Hendricks & E. Teller. J. Chem. Phys. 10 (1942) 147.

STUDIJ PROCESA GRAFITIZACIJE POMOĆU RENDGENSKIH DIFRAKCIJSKIH METODA

S. POPOVIĆ

Institut »Ruđer Bošković«, Zagreb

Sadržaj

Grijanjem praška petrolkoksa od 1000° C do 3000° C dobiven je niz uzoraka različite kristaliničnosti. Razmatra se mijenjanje mikrostrukturnih parametara uz promjenu temperature i diskutira postepeno moduliranje difrakcijskih linija tokom procesa grafitizacije. Povećanjem temperature iznad 1200° C početni međuslojni razmak d_{002} (3.47 Å) smanji se do vrijednosti (3.44 Å), koja je karakteristična za negrafitne karbone. Iznad 1600° C d_{002} smanjuje se vrlo polako i do 2150° C uzorci imaju nesređenu slojevitu strukturu. Iznad 2200° parovi najbližih susjednih slojeva počinju poprimati pravilni grafitni odnos i d_{002} se naglo smanjuje. Sređivanje slojeva uzrokuje moduliranje dvodimenzionalnih difrakcijskh (*hk*) *uz pojavu refleksa* (*hkl*). Dio volumena, koji sadržava nesređenu slojevitu strukturu i iznad 2200° C, bez promjene d_{002},, smanji se od 15% kod 2230° C na 5% kod 3000° C. U cijelom temperaturnom području povećava se veličina kristalita u smjeru okomitom na slojeve (L_c) i u smjeru paralelnom slojevima (L_a). Povećanje L_c je osobito veliko iznad 1900° C, a povećanje L_a iznad 2200° C. Prosječna distorzija kristalne rešetke smanjuje se porastom temperature, i to naročito brzo od 1600° C do 2100° C. Prostorno sređivanje najbližih susjednih parova slojeva ovisi o ostalim susjednim slojevima. Raspodjela orijentiranih i neorijentiranih slojeva u kristalima grafitne komponente ja kaotična iznad 2200° C.